Systematic Study of the Effect of Auxiliary Acceptors in D-A′-π-A Sensitizers Used on Dye Sensitized Solar Cells

Ping Li[†,‡], Houyu Zhang[‡,] Alessandro Troisi[*†]

[†]Department of Chemistry, University of Liverpool, Liverpool L69 3BX, UK

[‡]State Key Laboratory of Supramolecular Structure and Materials, Institute of Theoretical Chemistry, Jilin University, Changchun 130012, P. R. China

*Email: a.troisi@liverpool.ac.uk

Abstract

We perform a systematic quantum chemical investigation to elucidate the effect of auxiliary acceptors (A′) on the electronic properties of D-A′-π-A dyes used in dye sensitized solar cells. A large set of dyes (380) are considered to achieve robust conclusions. Our calculations indicate that the auxiliary acceptor modulates, as expected, the LUMO level of the dye except for very poor acceptors. More surprising, some auxiliary acceptors also modify the HOMO level of the dye and its excited states acting effectively as auxiliary donors as well. The study of the data set reveals that the effect of changing the π-bridges is highly systematic and predictable. Despite the variability in the geometry between the connected fragments, the frontier molecular orbital energy levels of dyes are very closely related to the energy levels of the component fragments, e.g. it is easy to predict the change in electronic structure of a dye due to the change of one of its constituents.

1. Introduction

Dye-sensitized solar cells (DSSCs) have become one of the most promising technologies for solar energy conversion because of abundant and low-cost materials and ease of fabrication.[1-2] As a crucial component of DSSC, the sensitizer is responsible for light-harvesting, charge separation at dye/semiconductor interface, and dye regeneration. Great efforts have been devoted to the development of efficient sensitizers to boost the power conversion efficiencies (PCEs) of DSSCs.[3-5] High-performance organic sensitizers usually feature a donor-π-bridge-acceptor (D-π-A) structures.[6-7] In 2011, Zhu et al.[8] proposed a concept of D-A′-π-A motif for designing a new generation of efficient and stable organic sensitizers. D-A′-π-A featured sensitizers in which an additional electron-

withdrawing conjugated unit is incorporated into the bridge acting as an auxiliary electron acceptor (A′) for tailoring molecular structures, modulating the energy levels, absorption spectra, and improving the photostability of sensitizers have become attractive.[9-10] Recently, the electron-withdrawing units of benzothiadiazole (BTD),[11-12] benzotriazole (BTZ),[13-14] quinoxaline (Qu)[15-17] and diketo-pyrrolopyrrole (DPP)[18-19] have been exploited as auxiliary acceptors for constructing efficient D-A′-π-A structures. With the effort of molecular engineering, a significant increase in the photovoltaic efficiency have been achieved from ~5% to greater than 10%, a record efficiency of 13.0% has been obtained with porphyrin sensitizers.[20]

In this work we perform a systematic computational investigation to elucidate the effect of auxiliary acceptors on the geometrical and electronic properties of dyes at a microscopic level. To achieve more robust conclusions we consider a large set of dyes and we study the role of alternative acceptors on different properties within the database. The potential of high throughput computational study has been verified already a number of times in the context of dye sensitized solar cells. The large-scale data mining of dye structures predicts the properties of dyes from surveying a representative set of chemical space with several molecular predictors which are experimentally validated.[21-23] An alternative use of a large database of computed property is to build a relation between molecular properties and experimental efficiency as attempted for example in refs. [24-26] This work belongs to the first group of study and a set of hypothetical dyes are considered in their electronic structures to identify trend and guide the design of materials within this class of compounds. The next section describes the methodology used to build a database of dye and corresponding electronic structure property. The results section will first consider the relation between the orbitals of the fragments composing the dyes and the orbitals of the dyes in terms of energy and composition of the orbitals. The optical absorption properties and their relation with the charge transfer character are also considered alongside properties known to control the charge recombination rate like the reorganization energy. The goal throughout is to identify trends and relevant exceptions to such trends.

2. Methods

There are three different components in the methodology, (i) the choice of the systems to be studied, (ii) a strategy to accelerate their geometry optimization, and (iii) the computation of a number of properties for each system. These are discussed below.

Construction of the database. To clarify the effect of auxiliary acceptors in the data base of D-A′-π-A systematically, it is desirable that the A′ are derived from a relatively uniform set, we considered the auxiliary acceptors listed in the reviews by Lu et al.[27] and Zhang et al.[28] The auxiliary acceptors including F atoms are excluded because of their known chemical instability.[29] Thus 38 auxiliary acceptors were considered. Two donors, triphenylamine (D1) and indoline (D2), have been considered to make sure that the results are not donor-specific and the common anchoring acceptor (A) was used for all considered dyes. The five mostly common benzene (π1), thiophene (π2), furan (π3), thieno[3, 2-b]thiophene (π4)[30-32] and cyclopentadithiophene (π5)[33-34] were used as π-bridges for the reason that the role of A′ may be influenced by the nature of bridges (their length and orbital energy levels).[35-36] The building blocks of 2 donors, 38 auxiliary acceptors, 5 π-bridges and 1 anchoring acceptor are presented in Fig. 1 and so the final data set contained 380 dyes with D-A′-π-A structures and the corresponding 10 dyes without auxiliary acceptors for comparison.

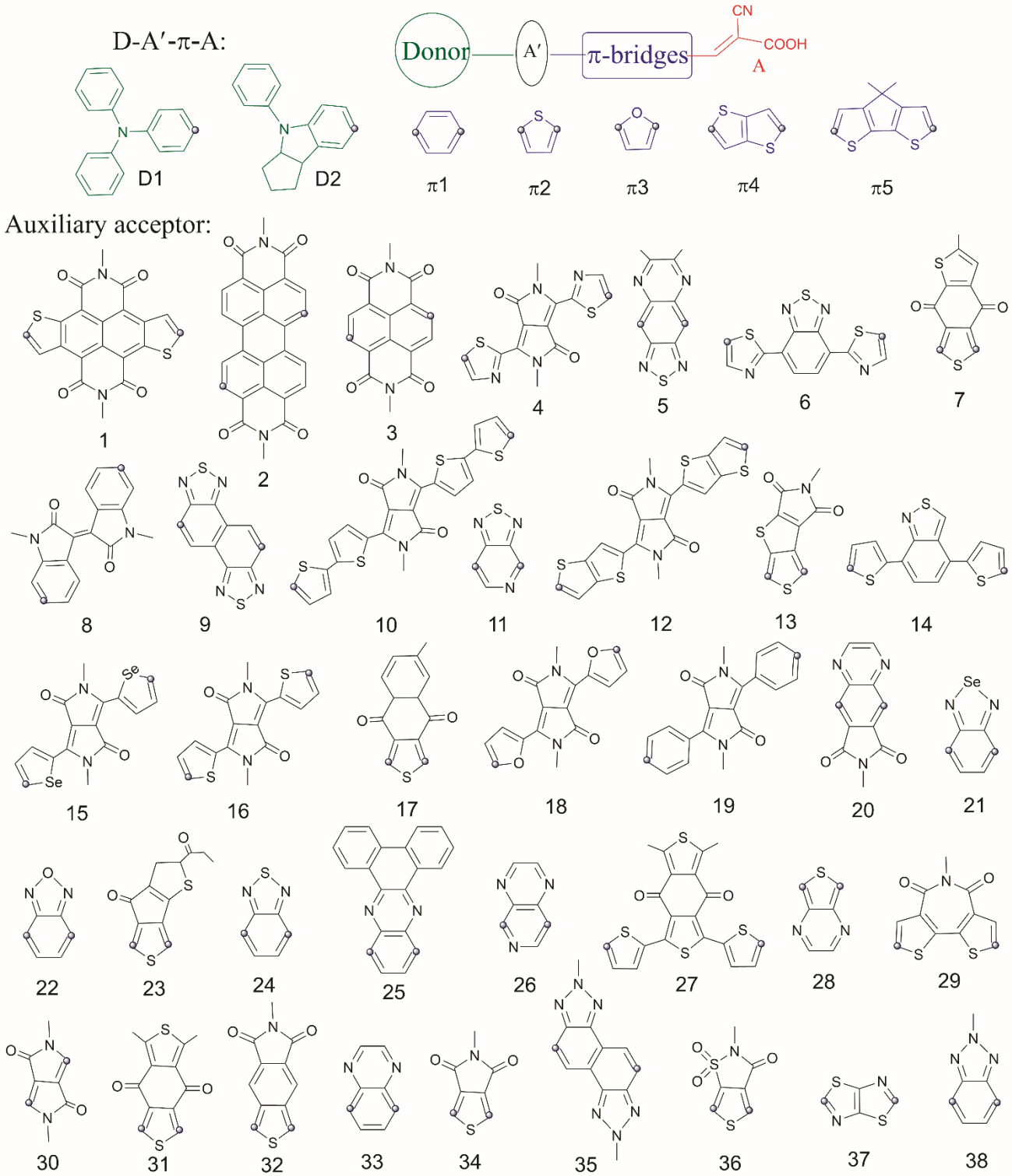

Figure 1. The building blocks used for generating the D-A′-π-A dyes. The points marked with circles represent the reactive sites in the generation process. For the A′ with two non-equivalent points, the left point is always connected to donor and the right always connected to π-bridge. The auxiliary acceptors are ordered by LUMO energy levels as discussed in the text.

Geometry optimization. Based on the optimized building blocks, we do the partial optimizations of arbitrary adjacent fragments in D-A′-π-A motif to obtain the desirable connection parameters (bonds,

angles and dihedrals), then we generate the library of dyes by linking the building blocks using the optimal connection parameters. The full geometry optimizations of dyes were done at B3LYP/6-31G* with a polarizable continuum model (PCM) to simulate the effect of acetonitrile solvent,[37-38] and frequency calculations were performed at the same level of theory to verify that the optimized geometry corresponds to a true potential energy minimum. The individual properties relevant to the power conversion efficiency of DSSC were calculated based on the stable optimized structures of dyes. The supporting information (SI, Table S1) reports the dihedral angles between D1/D2 and auxiliary acceptor, auxiliary acceptor and π1/π2 bridge, respectively. These vary substantially with average (standard deviation, SD) of 28.4 (12.9), 28.8 (16.2) [12.7 (17.7)] for the dihedral angles between D and A', A' and π1[π2], respectively.

Computed properties with corresponding computational details. We list below the properties computed and analyzed in this work, outline their importance for DSSC and show the computational method used.

(1) *HOMO-LUMO energy levels*. For the operation of TiO_2-DSSC device, the energy levels of HOMO and LUMO must fulfill the basic energetic requirements for efficient electron injection and dye regeneration, that is, the LUMO levels should be higher than the conduction band of TiO_2 (-4.0 eV)[39] and the HOMO levels should be lower than redox potential energy of I_3^-/I^- (-4.8 eV).[40] The majority of the discussion will be based on the relative shift of these orbital energy levels across the data set, so the systematic shifts are not sensitive to the absolute orbital levels reported for different functionals.[41-42]

(2) *Absorption spectra*. An ideal sensitizer should absorb solar radiation as much as possible in the visible-IR range to match the solar spectrum. The absorption spectra were simulated using TDDFT method at the CAM-B3LYP/6-31G* level with the inclusion of solvent. The functional of CAM-B3LYP has been proved to perform well in the description of charge-transfer excitations.[43-44] The maximum absorption wavelength (λ_{max}) and the corresponding oscillator strength are obtained from the first transition.

(3) *Free energy of dye oxidation in solution* (ΔG), defined by the equation below:

$$M^+_{(aq)} \xrightarrow{\Delta G} M_{(aq)} + e^-$$

The ground state oxidation potential of dyes in solution can be calculated with entropic contribution

evaluated from frequency calculation in the harmonic approximation. The frequencies were done based on the optimized dyes in their neutral ($M_{(aq)}$) and positively charged ($M^{+}_{(aq)}$) states at the B3LYP/6-31G* level in solution. It has been demonstrated that power conversion efficiency correlates strongly with the oxidation potential of dye. Usually high efficiencies are found in a certain range of oxidation potential.[25, 45]

(4) *Reorganization energy*. This quantity reflects the energy required for the structural relaxation of dyes upon charge transfer, including contributions from the inner reorganization energy (λ_{int}, which is induced by intramolecular vibrations) and the external reorganization energy (λ_{ext}, which is caused by polarization of surrounding medium). This parameter enters into the theory of interfacial electron transfer and determines the charge recombination rate to the oxidized dye nonlinearly.[45-46] It was computed at the same level used for ΔG (B3LYP/6-31G* in acetonitrile) following the procedure below. The λ_{int} is calculated directly from the relevant points on the adiabatic potential energy surfaces (PES) using the standard procedure:[47]

$$\lambda_{int} = \lambda_0 + \lambda_+ = (E_0^* - E_0) + (E_+^* - E_+)$$

where E_0 and E_+ represent the energies of the neutral and cation species in their lowest energy geometries, respectively, while E_0^* and E_+^* represent the energies of the neutral and cation species with the geometries of the cation and neutral species, respectively. The external reorganization energies is evaluated as:

$$\lambda_{ext} = \frac{1}{2}\left(E^{(1)}(M^+) - E^{(0)}(M^+)\right) + \frac{1}{2}(E^{(1)}(M) - E^{(0)}(M))$$

where E indicates the energy of particular electronic configuration: neutral molecule (M) or charged molecule (M^+). The superscript refers to the polarization of the continuum dielectric used to model the surrounding solvent. $E^{(0)}(M)$ and $E^{(0)}(M^+)$ indicate that the energy has been evaluated with the solvent polarization that stabilizes the neutral and positively charged molecule, respectively (A routine electronic structure calculation with PCM). $E^{(1)}(M)$ and $E^{(1)}(M^+)$ indicate that the energy has been evaluated with the solvent polarization that stabilizes positively charged and neutral molecule, respectively (not the state for which the energy is computed). This procedure was proposed and tested in refs.[48-49]

(5) *Difference between ground and excited state dipole moment ($\Delta\mu$).* In some dyes, the first excited state is characterized by a strong charge transfer character, which is believed to be beneficial for the

ultrafast interfacial electron injection from the sensitizer to the conduction band of TiO_2 and for the efficient charge neutralization of the dye.[50-51] Here, the intramolecular charge transfer character is described with the dipole difference ($\Delta\mu$) between the ground-state and first excited-state dipole moment of dyes, which is analyzed by using Multiwfn software.[52]

(6) *Orbital composition analysis*. The large weight of donor in the compositions of HOMO would be favorable for dye regeneration, and a large orbital density of the LUMO and a small orbital density of the HOMO on the anchoring acceptor would be benefit to facilitate electron injection and inhibit charge recombination, respectively.[53] We analyzed the orbital weighting by reporting the Mulliken population on the fragment of D, A′, π and A, respectively, which is done with Multiwfn software.

All calculations were performed with Gaussian16 package.[54]

3. Results

Study of the orbital levels of the isolated fragments composing the dyes. Dyes of the D-π-A or D-A′-π-A family are designed so that the HOMO is localized on the donor and the LUMO on the A (or A') fragment. In practice, as there is interaction between fragments the dye's orbitals can be more delocalized as a result of orbital mixing. This mixing is larger between fragment orbitals closer in energy. The first step to rationalize the dyes orbitals nature and energy is to consider the energy levels of the fragments. Fig. 2 reports the HOMO and LUMO energy levels of the isolated fragments. The auxiliary acceptors are conveniently ordered by the increased LUMO energy levels (the electron-withdrawing ability of A′ changing from strong to weak). A first relevant observation is that LUMO energy levels of auxiliary acceptors beyond acceptor number 30 are higher than that of the anchoring acceptor, i.e. one can anticipate that the LUMO of the dye is more localized on A′ for the acceptors until acceptor number ~30 and on A for the remaining weaker acceptors. Traditionally one does not pay much attention to the HOMO energy level of A′ but we show in the reminder of the paper that this can be important. It seems from Fig. 2 that there is no correlation between HOMO energy levels and the electron-withdrawing ability of auxiliary acceptors. Notably, the A′ tend to have similar energy of the HOMO with the π bridges and some of them (10, 12, 15, 16 and 18) have energy closer to the donors D1 and D2. Because of this energy alignment it is possible that the HOMO of the dye is influenced by these high-HOMO-energy auxiliary acceptors, as it will be seen below.

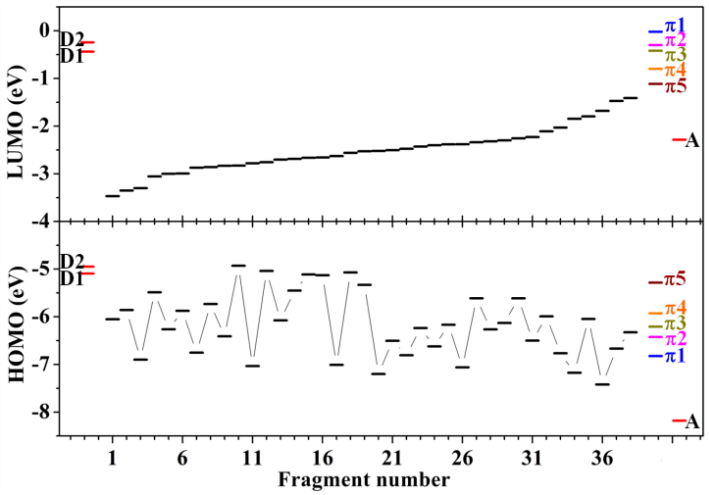

Figure 2. Calculated HOMO and LUMO energy levels for the isolated fragments. Donors, anchoring acceptor and π-bridge levels are labelled. The unlabeled levels refers to the 38 A′ at the corresponding coordinate in the horizontal axis.

Study of the orbital levels of the dyes. The calculated HOMO and LUMO energy levels of dyes are shown in Fig. 3. The first observation is that the trend of energy levels of dyes with D1 and D2 is so similar that we can conveniently focus on the dyes with D1 in the rest of article and report the properties of dyes with D2 in the SI. The LUMO energy level of dye rises obviously with the increasing LUMO of acceptor number 1-6 whose electron-withdrawing ability is significantly strong. Then the LUMO energy of dye slowly rises following the moderated LUMO energy of A′ (compare with Fig. 2) until acceptor number 30 where the LUMO becomes too high in comparison with the anchoring acceptor. The HOMO level of the dye is also modulated to some extent by A′, as shown in the bottom panels of Fig. 3. In particular, the high-HOMO-energy auxiliary acceptors (10, 12, 15, 16 and 18) cause the HOMO of the dyes to be appreciably larger. This was anticipated from the study of the fragment orbitals, but it was *a priori* not expected that auxiliary acceptors had an effect on the HOMO levels. To quantitatively evaluate the influence of auxiliary acceptors on the energy levels of dyes, the standard deviation was calculated and the variance of HOMO (SD of 0.11 eV) is only a bit smaller than that of LUMO (SD of 0.17 eV). In Table S1 of the SI we show that there is a large variation of the angle θ between the conjugation planes of the fragments which is associated to a large variation on the coupling between them (it depends on $\cos(\theta)$). However, because of the very strong correlation between the fragment's orbital energy and the energy of the dye's orbital it seems that the large variation of the interaction between fragments is not as critical as one may have anticipated and will not be discussed in the reminder of this work. Another interesting finding is that the effect of the bridge is quite systematic, e.g. a certain π-bridge tends to push the LUMO or HOMO level in the same

direction. This is particularly surprising for the LUMO level (very different in energy for the levels of the isolated bridge). The effect of the bridge will be analyzed in greater detail below.

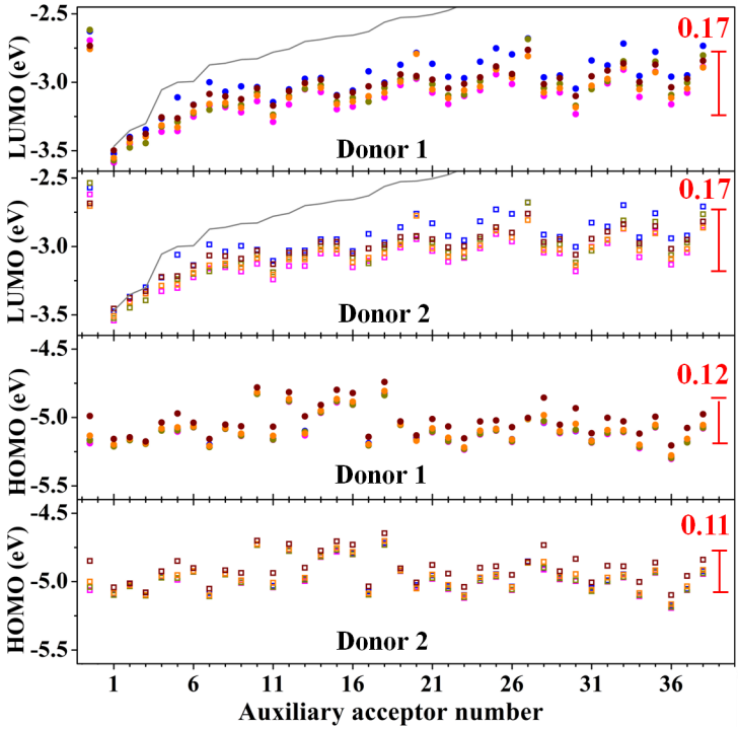

Figure 3. Calculated HOMO and LUMO energy levels for dyes with D1 (circle) and D2 (square) as donors. The leftmost data are for the D-π-A dyes without auxiliary acceptor. The 5 values on each value of the acceptor axis are for the dyes with different π-bridges (using the same color scheme of Fig. 2). The values in red are the standard deviation of energy levels of D-A′-π-A dyes changing auxiliary acceptors. The gray line in the top two panel show the LUMO energy of the isolated A′ fragment.

Relation between orbital levels, energy gap and redox potentials. The orbital energy levels of the whole database are plotted against the energy gap (E_{LUMO}-E_{HOMO}) in Fig. 4. It can be found that most of dyes meet the basic energetic requirement with respect to the TiO_2 conduction band and the I_3^-/I^- redox mediator, except for the dyes with high-HOMO-energy auxiliary acceptors (10, 12, 15, 16 and 18). The dyes with D2 (square) possess higher HOMO energy levels compared to the dyes with D1 (circle) because of the stronger electron-donating ability of D2. And the dyes with π1(blue) exhibit relatively larger E_{gap} might due to the distorted geometrical structures. The entire data set spans a range of 0.66 eV for HOMO, 0.91 eV for LUMO and 1.18 eV for E_{gap}. In Fig. S1 of the SI we show that there is an excellent correlation (Pearson correlation coefficient 0.99) between the computed HOMO energy levels and the oxidation potential (including solvent effect). For this reason we omit from the main manuscript the discussion of the oxidation potential that would mirror that of the HOMO.

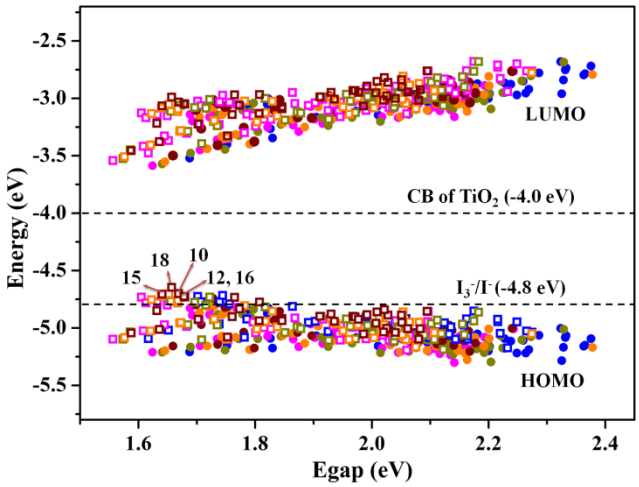

Figure 4. Calculated E_{HOMO} and E_{LUMO} relative to vacuum ordered by the resulting E_{gap} of dyes with D1 (circle) and D2 (square) as donors and π1(blue), π2(magenta), π3(dark yellow), π4(orange) and π5(wine) as π-bridges. The horizontal dashed lines represent the energy levels of conduction band (-4.0 eV) and redox mediator (-4.8 eV), respectively.

Composition of the frontier orbitals in terms of fragment contribution. To describe how the different fragments contribute to the frontier orbital of the dye, the percentage weight of each fragments in the composition of HOMO and LUMO is presented in Fig. 5. As expected the weight of A′ in the LUMO of dyes is gradually decreased as the acceptor strength decrease with increasing auxiliary acceptor number. The high-HOMO-acceptors (10, 12, 15, 16, 18) show substantially larger contribution to HOMO of the corresponding dyes, i.e., as predicted already from the orbital alignment, they participate to the HOMO as much as to the LUMO. The large Mulliken population of D to HOMO and A to LUMO would be favorable for dye regeneration and electron injection, respectively, and small A to HOMO would be benefit to inhibit charge recombination. However, a too strong auxiliary acceptor A′ may trap the electron upon photoexcitation. If the thermal energy is not high enough to drive the electron density from the auxiliary acceptor to the anchoring acceptor, the decreased LUMO population on both the π-bridges and A would slow down charge injection.[55-56]

Below we will further discuss the change in the orbital weight on the anchoring group to clarify the possible effects of changing A′ on the charge recombination rate at the interface.

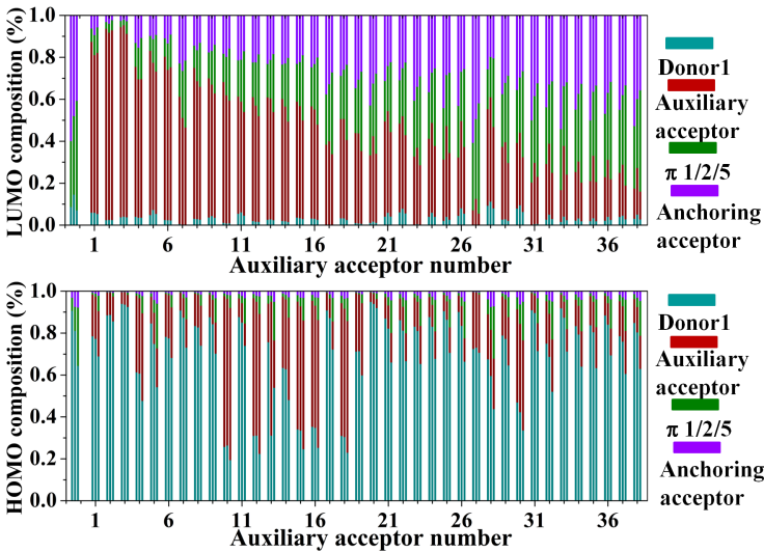

Figure 5. Fragment contribution to the composition of LUMO (top) and HOMO (bottom). The leftmost data are for the D-π-A dyes without auxiliary acceptor. In correspondence to each auxiliary acceptor number (along *x* axis) we report the values for the dyes with that acceptor and three different bridges (π1, π2, π5 from left to right).

Optical absorption properties. There are two main effects on the adjustment of maximum absorption wavelength of dyes. The data show that the effect of changing auxiliary acceptor (causing a shift of λ_{max} in the range from -53 to 223 nm, see Table S2) is larger than the effect of changing the π-bridge (shifting λ_{max} in the 3–129 nm range, see Table S3). The negative values indicate the dyes exhibit blue-shifted λ_{max} compared to the dyes without auxiliary acceptors.

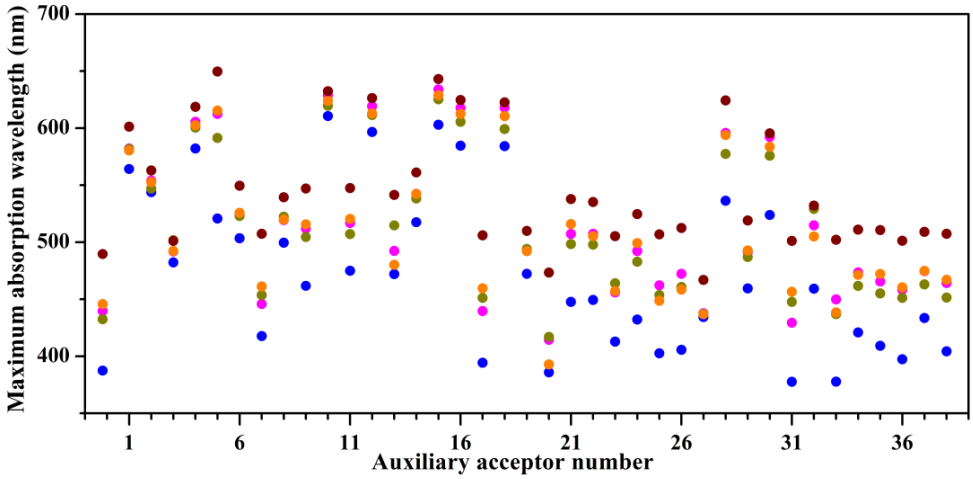

Figure 6. Calculated maximum absorption wavelength (λ_{max}) in the visible-near-IR range for the dyes with D1 (π1(blue), π2(magenta), π3(dark yellow), π4(orange) and π5(wine)). The data of first column in the left are for the D-π-A dyes without auxiliary acceptor.

Compared to the corresponding D-π-A dyes (the data in the first column in Fig. 6), most of the dyes

with A′ show red-shifted λ_{max}. A small red-shifted λ_{max} of dyes with additional auxiliary acceptor is expected for the reason that the longer molecules would cause red-shifted λ_{max}. However, some of the shift is more substantial, namely for the special dyes with A′ of 10, 12, 15, 16, and 18, for which we have noticed that the HOMO is dominated by A′ and has larger HOMO energy than the others. In these molecules, A′, which has the greatest weight in the population of both HOMO and LUMO, can be seen as an acceptor also as a donor and yield an electronic structure very different from that expected for a D-A′-π-A dye, where the HOMO is localized on D. In dyes where A′ has very high HOMO energy the structure described equally well by the notation D-D′-π-A, where the auxiliary acceptor is also an auxiliary donor. If we neglect these special cases the trend is approximately blue-shifted absorption with the increase of the LUMO energy (acceptor number) of A′ as expected. The effect of π-bridges on the absorptions is systematic. The dyes with π5 (in wine) exhibit consistently larger λ_{max} than that of dyes with π1 (in blue) , and further one can predict the blue-red shift character of the bridges.

Influence of the π-bridge on orbital levels. The systematic effect of π-bridges on shifting the orbital energy levels and optical absorption properties including maximum absorption wavelength and the corresponding oscillator strength of dyes are analyzed and shown in Fig. 7. The above properties are computed as described in section 2. For each property P_{ij}, for auxiliary acceptor *i* and bridge *j*, we evaluate the average value of that property across the different bridges $\overline{P_i} = \frac{1}{5}\sum_j P_{ij}$ and the deviation from the average $D_{ij} = P_i - \overline{P_i}$. Any systematic shift due to bridge *j* can be seen from the average shift $\overline{D_j} = \frac{1}{N_{A'}}\sum_i D_{ij}$ reported in Fig. 7 with the standard deviation $\sigma_j^2 = \frac{1}{N_{A'}}\sum_i (D_{ij} - \overline{D_j})^2$. The π1 decreases the HOMO and increases the LUMO energy level, resulting in larger HOMO-LUMO energy gap and blue-shifted absorption, however, π2-4 cause lightly red-shifted absorptions because of the declining in the LUMO is a little larger or the same as that of HOMO, an obvious red-shifted absorption is observed for π5 due to its extended conjugation property. The shift of absorption is basically consistent with the changing trend of energy levels of the isolated π-bridges. The oscillator strength at the maximum absorption wavelength is increasing following the order from π1 to π5, which might be attributed to the extended π-conjugation of π-bridges. It should be noted that the results of Fig. 7 become more significant thanks to the large set of data considered. Not only is it possible to predict the shift of a particular parameter due to a chemical change but also the probability distribution of a certain shift.

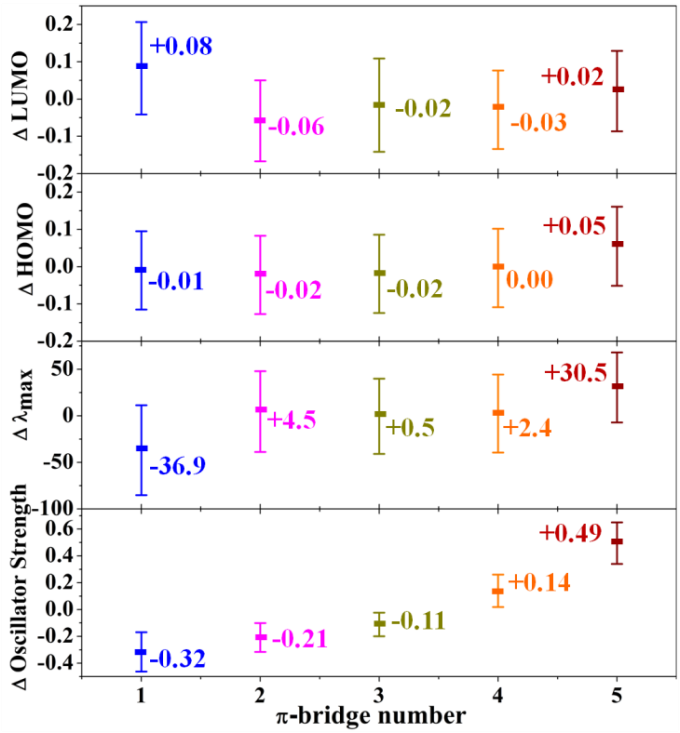

Figure 7. Systematic effect of π-bridges. (π1(blue), π2(magenta), π3(dark yellow), π4(orange) and π5(wine)).

Correlation between charge transfer character and absorption properties. Larger dipole moment difference (Δμ, a measure of charge transfer character) are expected to associate with decreased maximum absorption wavelength and oscillator strength (the latter is undesirable for a dye) and the expectations are confirmed by the data shown in Fig. 8. It can be found that the dyes with π5 (in wine) always are associated with smaller charge transfer character, while a larger CT character is an association of dyes with π1 (in blue). The extended π-conjugation (π5) may cause inefficient intramolecular charge separation and charge transfer, decreasing the CT character in the first excited-state absorption.

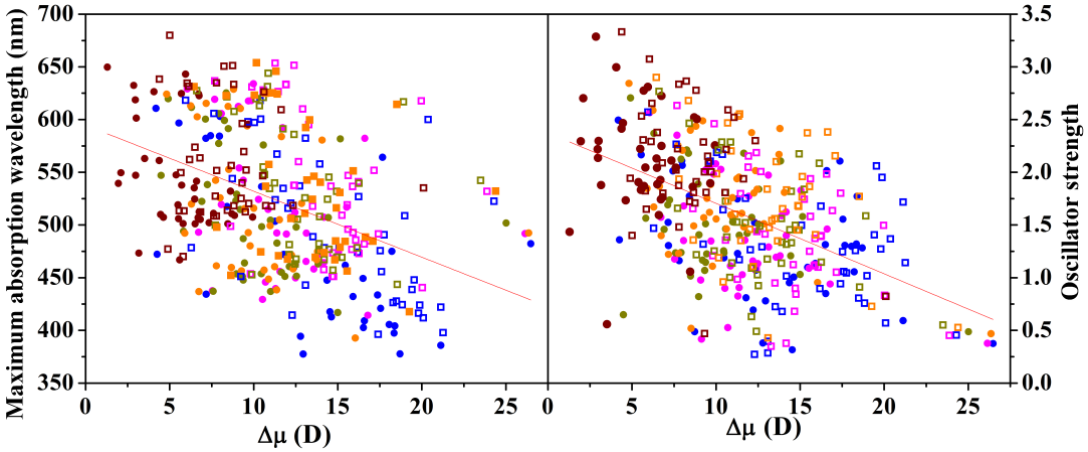

Figure 8. Correlation between dipole moment difference (Δμ) and maximum absorption wavelength (left), and Δμ and oscillator strength (right).

Effects influencing the charge transfer efficiency. We have also looked for systematic trends in the weight of anchoring acceptor in the compositions of HOMO and reorganization energy (internal or external), which are known to regulate the rate of charge recombination at the interface.[45] As shown in Fig. 9, the proportion of the HOMO distribution on the anchoring acceptor is affected by π-bridge, which is not correlated with HOMO energy of dyes. The dyes with π1 exhibit the smallest HOMO composition in A suggesting relatively reduced charge recombination. Compared to the corresponding D-π-A dyes, the dyes with additional auxiliary acceptors possess smaller HOMO distribution on A. However, the D-A′-π-A dyes own fairly stable total reorganization energies compared to the corresponding D-π-A dyes, so the auxiliary acceptor does not influence the charge recombination rate via modulation of the reorganization energy.

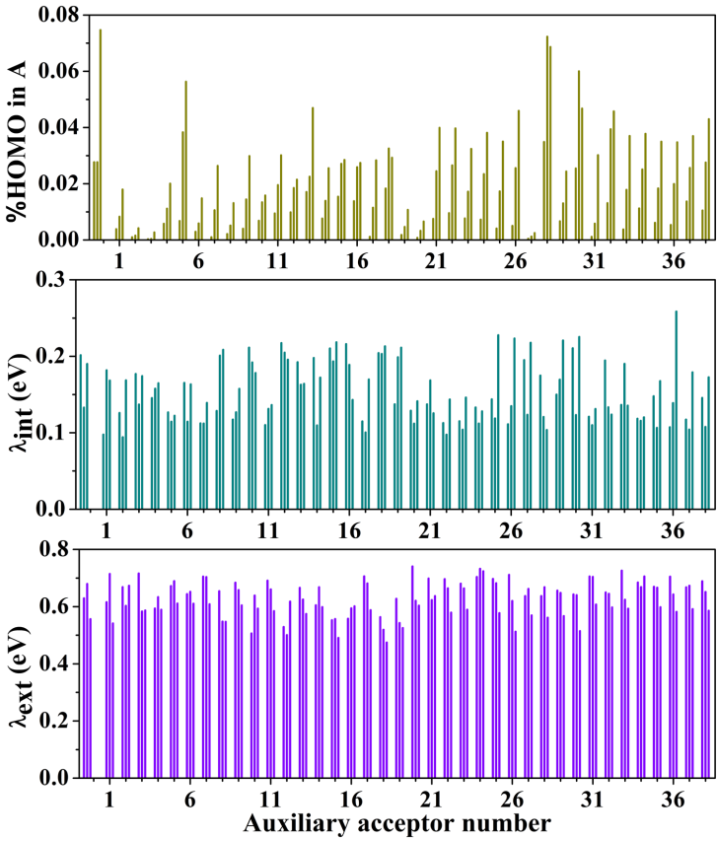

Figure 9. Calculated HOMO composition in anchoring acceptor (A) (top), inner (middle) and external (bottom) reorganization energy for the dyes with D1. The values on each number of x axis are for the dyes with π 1/2/5 bridges. The leftmost data are for the D-π-A dyes without auxiliary acceptor.

4. Conclusion

In this work, we present a systematic theoretical study on the D-A′-π-A dyes with various auxiliary acceptors. By comparing the orbital energy levels of isolated fragments and dyes, we can find that the

LUMO energy of the dye relatively follows the LUMO energy of A′, and that the HOMO level is also (more moderately) modulated by changing A′, especially when A′ has some donor characteristics (high HOMO energy). These trends are mirrored by the change in composition of the HOMO and LUMO of the dye expressed in terms of the density on each fragment. Generally most D-A′-π-A dyes show blue-shifted absorption with the increase of the LUMO energy (acceptor number) of A′ as expected. An interesting feature of this family of materials is that certain high-HOMO-energy A′ fragments completely modify the nature of the HOMO of the dye (that becomes centered on A′) and the nature of the first excited states which is significantly red-shifted: the D-A′-π-A have been turned into D-D′-π-A dyes and, strictly speaking, the dyes do not belong to the same chemical class. Particularly significant for the ability to fine tune the properties of these dyes is the very systematic behavior observed on the HOMO-LUMO energy levels, molecular orbital composition, maximum absorption wavelength and oscillator strength when the π-bridge is modified. Electronic effect seems to dominate over geometric effects and also the reorganization energy is fairly stable across the range of considered compounds. All these key findings have been possible because of the large data set considered suggesting that they can be applied beyond the specific data set considered to predict how the electronic structure of a dye would change as a result of changing the π-bridge or the auxiliary acceptor. More generally, a similar analysis can be used to rationalize the change of any low band-gap molecular materials generated from a library of constituent fragments.

Supporting Information

Correlation between HOMO energy levels and oxidation free energy, calculated fragment contribution to the composition of HOMO and LUMO, the maximum absorption wavelength (λ_{max}), the inner and external reorganization energy for the dyes with D2, the original data of maximum absorption wavelength of dyes.

Acknowledgements

P.L. acknowledges the support of the China Scholarship Council (No. 201706170217). A.T. acknowledge ERC grant No. 615834.

References:

1. O'Regan, B.; Grätzel, M., A Low-Cost, High-Efficiency Solar Cell Based on Dye-Sensitized Colloidal TiO_2 Films. *Nature* **1991,** *353*, 737.
2. Hagfeldt, A.; Boschloo, G.; Sun, L.; Kloo, L.; Pettersson, H., Dye-Sensitized Solar Cells. *Chem. Rev.* **2010,** *110*, 6595-6663.
3. Yella, A.; Lee, H.-W.; Tsao, H. N.; Yi, C.; Chandiran, A. K.; Nazeeruddin, M. K.; Diau, E. W.-G.; Yeh, C.-Y.; Zakeeruddin, S. M.; Grätzel, M., Porphyrin-Sensitized Solar Cells with Cobalt (Ii/Iii)–Based Redox Electrolyte Exceed 12 Percent Efficiency. *Science* **2011,** *334*, 629-634.
4. Clifford, J. N.; Martínez-Ferrero, E.; Viterisi, A.; Palomares, E., Sensitizer Molecular Structure-Device Efficiency Relationship in Dye Sensitized Solar Cells. *Chem. Soc. Rev.* **2011,** *40*, 1635-1646.
5. Yao, Z.; Zhang, M.; Wu, H.; Yang, L.; Li, R.; Wang, P., Donor/Acceptor Indenoperylene Dye for Highly Efficient Organic Dye-Sensitized Solar Cells. *J. Am. Chem. Soc.* **2015,** *137*, 3799-3802.
6. Ji, J.-M.; Zhou, H.; Kim, H. K., Rational Design Criteria for D–π–A Structured Organic and Porphyrin Sensitizers for Highly Efficient Dye-Sensitized Solar Cells. *J. Mater. Chem. A* **2018,** *6*, 14518-14545.
7. Liang, M.; Chen, J., Arylamine Organic Dyes for Dye-Sensitized Solar Cells. *Chem. Soc. Rev.* **2013,** *42*, 3453-3488.
8. Zhu, W.; Wu, Y.; Wang, S.; Li, W.; Li, X.; Chen, J.; Wang, Z.S.; Tian, H., Organic D-A-π-A Solar Cell Sensitizers with Improved Stability and Spectral Response. *Adv. Funct. Mater.* **2010,** *21*, 756-763.
9. Velusamy, M.; Justin Thomas, K. R.; Lin, J. T.; Hsu, Y.-C.; Ho, K.-C., Organic Dyes Incorporating Low-Band-Gap Chromophores for Dye-Sensitized Solar Cells. *Org. Lett.* **2005,** *7*, 1899-1902.
10. Wu, Y.; Zhu, W.-H.; Zakeeruddin, S. M.; Grätzel, M., Insight into D-A-π-A Structured Sensitizers: A Promising Route to Highly Efficient and Stable Dye-Sensitized Solar Cells. *ACS Appl. Mater. Interfaces* **2015,** *7*, 9307-9318.
11. Wu, Y.; Zhang, X.; Li, W.; Wang Z.; Tian H.; Zhu W., Hexylthiophene-Featured D–A–π–A Structural Indoline Chromophores for Coadsorbent-Free and Panchromatic Dye-Sensitized Solar Cells. *Adv. Energy Mater.* **2012,** *2*, 149-156.
12. Zhu, H.; Li, W.; Wu, Y.; Liu, B.; Zhu, S.; Li, X.; Agren, H.; Zhu, W., Insight into Benzothiadiazole Acceptor in D–A−π–A Configuration on Photovoltaic Performances of Dye-Sensitized Solar Cells. *ACS Sustainable Chem. Eng.* **2014,** *2*, 1026-1034.
13. Mao J.; Guo F.; Ying W.; Wu W.; Li J.; Hua J., Benzotriazole-Bridged Sensitizers Containing a Furan Moiety for Dye-Sensitized Solar Cells with High Open-Circuit Voltage Performance. *Chem.- Asian J.* **2012,** *7*, 982-991.
14. Cui, Y.; Wu, Y.; Lu, X.; Zhang, X.; Zhou, G.; Miapeh, F. B.; Zhu, W.; Wang, Z.-S., Incorporating Benzotriazole Moiety to Construct D–A−π–a Organic Sensitizers for Solar Cells: Significant Enhancement of Open-Circuit Photovoltage with Long Alkyl Group. *Chem. Mater.* **2011,** *23*, 4394-4401.
15. Pei, K.; Wu, Y.; Islam, A.; Zhang, Q.; Han, L.; Tian, H.; Zhu, W., Constructing High-Efficiency D–A−π–A-Featured Solar Cell Sensitizers: A Promising Building Block of 2,3-Diphenylquinoxaline for Antiaggregation and Photostability. *ACS Appl. Mater. Interfaces* **2013,** *5*, 4986-4995.
16. Pei K.; Wu Y.; Wu W.; Zhang Q.; Chen B.; Tian H.; Zhu W., Constructing Organic D–A–π-A-Featured Sensitizers with a Quinoxaline Unit for High-Efficiency Solar Cells: The Effect of an Auxiliary Acceptor on the Absorption and the Energy Level Alignment. *Chem. -Eur. J.* **2012,** *18*, 8190-8200.
17. Zhang, W.; Wu, Y.; Bahng, H. W.; Cao, Y.; Yi, C.; Saygili, Y.; Luo, J.; Liu, Y.; Kavan, L.; Moser, J.-E.; Hagfeldt, A.; Tian, H.; Zakeeruddin, S. M.; Zhu, W.-H.; Grätzel, M., Comprehensive Control of Voltage Loss Enables 11.7% Efficient Solid-State Dye-Sensitized Solar Cells. *Energy Environ. Sci.* **2018,** *11*, 1779-1787.
18. Qu, S.; Qin, C.; Islam, A.; Wu, Y.; Zhu, W.; Hua, J.; Tian, H.; Han, L., A Novel D-A-π-A Organic Sensitizer Containing a Diketopyrrolopyrrole Unit with a Branched Alkyl Chain for Highly Efficient and Stable Dye-Sensitized Solar Cells. *Chem. Commun.* **2012,** *48*, 6972-6974.
19. Qu, S.; Wu, W.; Hua, J.; Kong, C.; Long, Y.; Tian, H., New Diketopyrrolopyrrole (DPP) Dyes for Efficient Dye-

Sensitized Solar Cells. *J. Phys. Chem. C* **2010,** *114*, 1343-1349.

20. Mathew, S.; Yella, A.; Gao, P.; Humphry-Baker, R.; Curchod, B. F. E.; Ashari-Astani, N.; Tavernelli, I.; Rothlisberger, U.; Nazeeruddin, M. K.; Grätzel, M., Dye-Sensitized Solar Cells with 13% Efficiency Achieved through the Molecular Engineering of Porphyrin Sensitizers. *Nature Chem.* **2014,** *6*, 242.

21. Cole, J. M.; Low, K. S.; Ozoe, H.; Stathi, P.; Kitamura, C.; Kurata, H.; Rudolf, P.; Kawase, T., Data Mining with Molecular Design Rules Identifies New Class of Dyes for Dye-Sensitised Solar Cells. *Phys. Chem. Chem. Phys.* **2014,** *16*, 26684-26690.

22. Li, Z.; Omidvar, N.; Chin, W. S.; Robb, E.; Morris, A.; Achenie, L.; Xin, H., Machine-Learning Energy Gaps of Porphyrins with Molecular Graph Representations. *J. Phys. Chem. A* **2018,** *122*, 4571-4578.

23. Ornso, K. B.; Pedersen, C. S.; Garcia-Lastra, J. M.; Thygesen, K. S., Optimizing Porphyrins for Dye Sensitized Solar Cells Using Large-Scale Ab Initio Calculations. *Phys. Chem. Chem. Phys.* **2014,** *16*, 16246-16254.

24. Venkatraman, V.; Foscato, M.; Jensen, V. R.; Alsberg, B. K., Evolutionary De Novo Design of Phenothiazine Derivatives for Dye-Sensitized Solar Cells. *J. Mater. Chem. A* **2015,** *3*, 9851-9860.

25. Ip, C. M.; Eleuteri, A.; Troisi, A., Predicting with Confidence the Efficiency of New Dyes in Dye Sensitized Solar Cells. *Phys. Chem. Chem. Phys.* **2014,** *16*, 19106-19110.

26. Sara, T.; Maurizio Mastropasqua, T.; Antonio, C.; Mariachiara, P.; Filippo De, A., Benchmarking DFT and Semi-Empirical Methods for a Reliable and Cost-Efficient Computational Screening of Benzofulvene Derivatives as Donor Materials for Small-Molecule Organic Solar Cells. *J. Phys.: Condens. Mat.* **2016,** *28*, 074005.

27. Lu, L.; Zheng, T.; Wu, Q.; Schneider, A. M.; Zhao, D.; Yu, L., Recent Advances in Bulk Heterojunction Polymer Solar Cells. *Chem. Rev.* **2015,** *115*, 12666-12731.

28. Zhang, X.; Grätzel, M.; Hua, J., Donor Design and Modification Strategies of Metal-Free Sensitizers for Highly-Efficient n-Type Dye-Sensitized Solar Cells. *Front. Optoelectron.* **2016,** *9*, 3-37.

29. Sivasubramaniam, V.; Brodkorb, F.; Hanning, S.; Loebl, H. P.; van Elsbergen, V.; Boerner, H.; Scherf, U.; Kreyenschmidt, M., Fluorine Cleavage of the Light Blue Heteroleptic Triplet Emitter Firpic. *J. Fluor. Chem.* **2009,** *130*, 640-649.

30. Bong-Gi, K.; Chang-Gua, Z.; Jeong, J. E.; John, K.; Jinsang, K., Organic Dye Design Tools for Efficient Photocurrent Generation in Dye-Sensitized Solar Cells: Exciton Binding Energy and Electron Acceptors. *Adv. Funct. Mater.* **2012,** *22*, 1606-1612.

31. Wang, J.; Li, H.; Ma, N.-N.; Yan, L.-K.; Su, Z.-M., Theoretical Studies on Organoimido-Substituted Hexamolybdates Dyes for Dye-Sensitized Solar Cells (DSSC). *Dyes Pigments* **2013,** *99*, 440-446.

32. Zhang, G.; Bala, H.; Cheng, Y.; Shi, D.; Lv, X.; Yu, Q.; Wang, P., High Efficiency and Stable Dye-Sensitized Solar Cells with an Organic Chromophore Featuring a Binary π-Conjugated Spacer. *Chem. Commun.* **2009**, 2198-2200.

33. Li, R.; Liu, J.; Cai, N.; Zhang, M.; Wang, P., Synchronously Reduced Surface States, Charge Recombination, and Light Absorption Length for High-Performance Organic Dye-Sensitized Solar Cells. *J. Phys. Chem. B* **2010,** *114*, 4461-4464.

34. Cai, N.; Moon, S.-J.; Cevey-Ha, L.; Moehl, T.; Humphry-Baker, R.; Wang, P.; Zakeeruddin, S. M.; Grätzel, M., An Organic D-π-A Dye for Record Efficiency Solid-State Sensitized Heterojunction Solar Cells. *Nano Lett.* **2011,** *11*, 1452-1456.

35. Zhang, C.-R.; Liu, L.; Zhe, J.-W.; Jin, N.-Z.; Ma, Y.; Yuan, L.-H.; Zhang, M.-L.; Wu, Y.-Z.; Liu, Z.-J.; Chen, H.-S., The Role of the Conjugate Bridge in Electronic Structures and Related Properties of Tetrahydroquinoline for Dye Sensitized Solar Cells. *Int. J. Mol. Sci.* **2013,** *14*, 5461-5481.

36. Yigit, M. Z.; Bilgili, H.; Sefer, E.; Demic, S.; Zafer, C.; Can, M.; Koyuncu, S., Effect of a π-Bridging Unit in Triphenylamine-Benzothiadiazole Based Donor Acceptor Chromophores for Dye-Sensitized Solar Cells. *Electrochim. Acta* **2014,** *147*, 617-625.

37. Tomasi, J.; Mennucci, B.; Cammi, R., Quantum Mechanical Continuum Solvation Models. *Chem. Rev.* **2005,** *105*, 2999-3094.
38. Barone, V.; Cossi, M., Quantum Calculation of Molecular Energies and Energy Gradients in Solution by a Conductor Solvent Model. *J. Phys. Chem. A* **1998,** *102*, 1995-2001.
39. Grätzel, M., Photoelectrochemical Cells. *Nature* **2001,** *414*, 338.
40. Hagfeldt, A.; Grätzel, M., Light-Induced Redox Reactions in Nanocrystalline Systems. *Chem. Rev.* **1995,** *95*, 49-68.
41. Zhang, G.; Musgrave, C. B., Comparison of DFT Methods for Molecular Orbital Eigenvalue Calculations. *J. Phys. Chem. A* **2007,** *111*, 1554-1561.
42. Flores, F.; Ortega, J.; Vazquez, H., Modelling Energy Level Alignment at Organic Interfaces and Density Functional Theory. *Phys. Chem. Chem. Phys.* **2009,** *11*, 8658-8675.
43. Dev, P.; Agrawal, S.; English, N. J., Determining the Appropriate Exchange-Correlation Functional for Time-Dependent Density Functional Theory Studies of Charge-Transfer Excitations in Organic Dyes. *J. Chem. Phys.* **2012,** *136*, 224301.
44. Caricato, M.; Trucks, G. W.; Frisch, M. J.; Wiberg, K. B., Oscillator Strength: How Does TDDFT Compare to EOM-CCSD? *J. Chem. Theory Comput.* **2011,** *7*, 456-466.
45. Maggio, E.; Martsinovich, N.; Troisi, A., Evaluating Charge Recombination Rate in Dye-Sensitized Solar Cells from Electronic Structure Calculations. *J. Phys. Chem. C* **2012,** *116*, 7638-7649.
46. Bisquert, J.; Marcus, R. A., *Device Modeling of Dye-Sensitized Solar Cells. In Multiscale Modelling of Organic and Hybrid Photovoltaics*, Beljonne, D.; Cornil, J., Eds. Springer Berlin Heidelberg: Berlin, Heidelberg, 2014; pp 325-395.
47. Hutchison, G. R.; Ratner, M. A.; Marks, T. J., Hopping Transport in Conductive Heterocyclic Oligomers: Reorganization Energies and Substituent Effects. *J. Am. Chem. Soc.* **2005,** *127*, 2339-2350.
48. Li, X.-Y.; Tong, J.; He, F.-C., Ab Initio Calculation for Inner Reorganization Energy of Gas-Phase Electron Transfer in Organic Molecule–Ion Systems. *Chem. Phys.* **2000,** *260*, 283-294.
49. Jagoda-Cwiklik, B.; Slavíček, P.; Cwiklik, L.; Nolting, D.; Winter, B.; Jungwirth, P., Ionization of Imidazole in the Gas Phase, Microhydrated Environments, and in Aqueous Solution. *J. Phys. Chem. A* **2008,** *112*, 3499-3505.
50. Carsten, D.; Thomas, S.; Vladimir, D., Role of the Charge Transfer State in Organic Donor–Acceptor Solar Cells. *Adv. Mater.* **2010,** *22*, 4097-4111.
51. Zhang, J.; Li, H.-B.; Sun, S.-L.; Geng, Y.; Wu, Y.; Su, Z.-M., Density Functional Theory Characterization and Design of High-Performance Diarylamine-Fluorene Dyes with Different π Spacers for Dye-Sensitized Solar Cells. *J. Mater. Chem.* **2012,** *22*, 568-576.
52. Lu T.; Chen F., Multiwfn: A Multifunctional Wavefunction Analyzer. *J. Comput. Chem.* **2012,** *33*, 580-592.
53. Ding, W.-L.; Wang, D.-M.; Geng, Z.-Y.; Zhao, X.-L.; Yan, Y.-F., Molecular Engineering of Indoline-Based D–A−π–A Organic Sensitizers toward High Efficiency Performance from First-Principles Calculations. *J. Phys. Chem. C* **2013,** *117*, 17382-17398.
54. Frisch, M. J.; Trucks, G. W.; Schlegel, H. B.; Scuseria, G. E.; Robb, M. A.; Cheeseman, J. R.; Scalmani, G.; Barone, V.; Petersson, G. A.; Nakatsuji, H.; Li, X.; Caricato, M.; Marenich, A. V.; Bloino, J.; Janesko, B. G.; Gomperts, R.; Mennucci, B.; Hratchian, H. P.; Ortiz, J. V.; Izmaylov, A. F.; Sonnenberg, J. L.; Williams-Young, D.; Ding, F.; Lipparini, F.; Egidi, F.; Goings, J.; Peng, B.; Petrone, A.; Henderson, T.; Ranasinghe, D.; Zakrzewski, V. G.; Gao, J.; Rega, N.; Zheng, G.; Liang, W.; Hada, M.; Ehara, M.; Toyota, K.; Fukuda, R.; Hasegawa, J.; Ishida, M.; Nakajima, T.; Honda, Y.; Kitao, O.; Nakai, H.; Vreven, T.; Throssell, K.; Montgomery, Jr., J. A.; Peralta, J. E.; Ogliaro, F.; Bearpark, M. J.; Heyd, J. J.; Brothers, E. N.; Kudin, K. N.; Staroverov, V. N.; Keith, T. A.; Kobayashi, R.; Normand, J.; Raghavachari, K.; Rendell, A. P.; Burant, J. C.; Iyengar, S. S.; Tomasi, J.; Cossi, M.; Millam, J. M.; Klene, M.; Adamo, C.; Cammi, R.; Ochterski, J. W.; Martin, R. L.; Morokuma, K.; Farkas, O.; Foresman, J. B.; Fox, D. J. *Gaussian 16 Rev. B.01*, Wallingford, CT, 2016.
55. Yen, Y.-S.; Chou, H.-H.; Chen, Y.-C.; Hsu, C.-Y.; Lin, J. T., Recent Developments in Molecule-Based Organic

Materials for Dye-Sensitized Solar Cells. *J. Mater. Chem.* **2012,** *22*, 8734-8747.
56. Chiu, C.-C.; Sheng, Y.-C.; Lin, W.-J.; Juwita, R.; Tan, C.-J.; Tsai, H.-H. G., Effects of Internal Electron-Withdrawing Moieties in D–A−π–A Organic Sensitizers on Photophysical Properties for DSSCs: A Computational Study. *ACS Omega* **2018,** *3*, 433-445.

TOC Graphic: